Hydroxylation of alkanes by hydrogen peroxide in superacid: A superelectrophilic active intermediate and an ionization–hydration process

Hongchang Shi[*], Yilei Wang, Zhiguo Zhang

Department of Chemistry, Tsinghua University, Beijing 100084, China

Abstract

The density functional theory (DFT) at the B3LYP/6-311G(d,p) level was used to study the mechanism of hydroxylation of alkanes by hydrogen peroxide in superacid. Calculation showed that the hydroxylation of alkanes is an ionization–hydration process. The protonation of HOOH in superacid is the key to oxidation because it produces a superelectrophilic active intermediate ($HOOH_2^+$). The LUMO of $HOOH_2^+$ has much lower energy (-9.18 eV) than that (0.21 eV) of neutral HOOH. The energy (-9.18 eV) is approximately the same as or even at a lower level than the HOMO energy (-10.8 to -8.0 eV) of alkanes, which facilities nucleophilic transfer of σ electrons of alkanes toward the σ^* orbital of peroxo bonds. The electrophilic oxygen atom in $HO–OH_2^+$ is the oxygen in the –OH group. The attack target of the oxygen atom is the hydrogen atom of C–H. An IRC calculation revealed that the hydroxylation process is as follows: alkane is first ionized into a carbocation through a hydride transfer toward $HOOH_2^+$ and two H_2O molecules are formed. Then hydration of the carbocation with one H_2O molecule produces a protonated alcohol. The IRC also revealed that the microscopic nature of the hydroxylation is nucleophilic transfer of σ-electrons of a –C–H bond of alkanes toward the σ^* orbital of the peroxo bond of $HOOH_2^+$. For the hydroxylation of methane and ethane, the activation barriers are 2.58 and 1.40 kcal/mol, respectively. However, for hydroxylation of the secondary carbon of propane and the tertiary carbon of isobutane, the hydroxylation is a spontaneous process because the activity barriers have not appeared. For the hydroxylations of the primary carbons of propane and isobutene, although their activation barriers exist, they are extremely low (in the range of 0.1–1.4 kcal/mol). These results can explain why at very low temperature, even at $-78\,^{\circ}C$, alkanes could be oxidized by hydrogen peroxide in superacid and could produce various oxides.
© 2006 Elsevier B.V. All rights reserved.

Keywords: Alkane; Hydrogen peroxide; Hydroxylation; Ionization; Hydration

1. Introduction

The hydroxylation of alkanes by hydrogen peroxide in superacids, especially its oxidation mechanism, has been the focus of much research in the field of organic chemistry.

Alder and Whiting [1] first observed the reaction of alkanes with 85% hydrogen peroxide in hydrogen fluoride/boron trifluoride, but they considered it to be exceptionally destructive and unselective.

Frommer and Ulrich [2] reported that the hydroxylation of alkanes with 85% H_2O_2 in the presence of trifluoroacetic acid at 20 °C gives the corresponding alcohol.

Olah and coworkers [3(a)] systematically researched the oxidation of straight chain or branch chain alkanes by hydrogen peroxide in superacid. Their study showed that methane and ethane can be oxidized into a unitary hydroxylation product, methanol and ethanol. However, other alkanes, especially branch chain alkanes, at −78 °C also can be oxidized and used to produce varied oxides. From the products obtained in the reactions, the relative order of reactivity of single bonds in alkane was found to be $R_3C–H > R_2HC–H > RH_2C–H > H_3C–H > C–C$.

Regarding the mechanism of the oxidation by HOOH in superacids, Olah et al. [3,4] suggested a model in which a strong electrophilic HO^+ ion directly attacks the –C–H bond. HOOH in strong acid was expected to be protonated giving the hydroperoxonium ion $HOOH_2^+$. The strong electrophile was considered to be the source of the incipient HO^+ ion. The HO^+ directly attacks and is inserted into a –C–H bond of alkane that forms a

[*] Corresponding author. Tel.: +86 10 6278 3878; fax: +86 10 6277 1149.
*E-mail address:* shihc@mail.tsinghua.edu.cn (H. Shi).
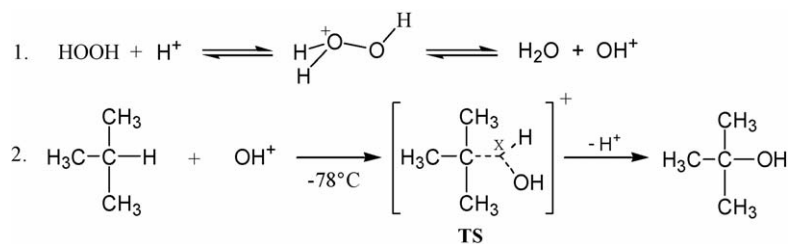
Scheme 1. Mechanism of hydroxylation of alkanes by HOOH in superacids proposed by Olah.

pentacoordinate carbocation involving 3c–2e (3 centers–2 electrons) C–H bond insertion as illustrated in Scheme 1, which shows the process for the hydroxylation of isobutane. However, there are obvious questions about the mechanism. (1) This is not a pentacoordinate carbocation, but still is a tetracoordinate carbocation (Scheme 1 TS) because HO··· and H··· are joined together and then one single bond connects to the carbon atom. (2) This also is not a 3c–2e C–H bond, but a 4c–2e bond because it increased the center X (Scheme 1, X in TS). The X is a non-nuclear or a virtual nucleus. Any bonding in molecules or intermediates should be a connection between atomic nucleuses, but should not be a combination with a virtual nucleus. Therefore, we consider that the mechanistic description is inexact at best.

The explorations of the mechanisms of many chemical reactions often are not enough when they rely only the results of experiments. Since the 1960s, quantum chemical calculation has become increasingly important tool in clarifying the mechanisms of chemical reactions.

In the last 20 years quantum chemists [5,6] have carried on unremitting efforts for exploring the hydroxylation mechanism of alkanes by hydrogen peroxide in superacid. Their calculation method usually was *ab initio*. Up to 1993, Schreiner et al. [5] have studied the reaction of NO$^+$ with methane. The calculation results by the *ab initio* method showed that the electrophilic attack of NO$^+$ is direct toward the atoms (H or C) rather than the C–H or C–C bonds. This conclusion disproved Olah's insertion pattern and was consistent with our results obtained by DFT calculation. However, Schreiner et al. hold that the oxidation process of methane is that the tetrahedral molecule is distorted to Cs symmetry (Scheme 2) and NO$^+$ directly attacks the nonbonding electron pair on the carbon atom. The distortion is an extremely energetic process, which is in need of energy of
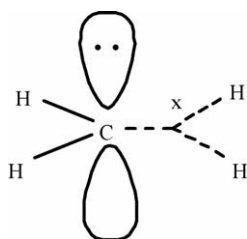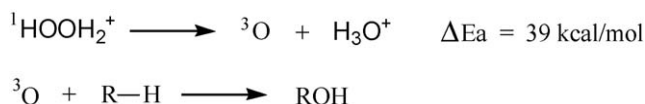
over 100 kcal/mol. The structure is not normal because a virtual nucleus (X) is also produced. Therefore, it is hard to believe the validity of the model would be confirmed by experimental facts.

At the same time Bach et al. [6(a,b)] suggested a frontier molecular orbital (FMO) model for electrophilic oxygen atom insertion into saturated hydrocarbons. According to the model, the hydroxylation first requires a 1,2-hydrogen shift in HOOH or HOOH$_2$$^+$ to afford water oxide H$_2$OO or HO$^+$. Then the oxide attacks the carbon atom of alkanes and approaches it along the orientation of the approximate atomic 2p carbon orbital to complete the hydroxylation. The calculations were conducted using *ab initio* method at MP$_2$, MP$_4$, QCISD, QCISD(T), CASSCI, and MRCI level. However, the 1, 2-hydrogen shift must overcome 30–50 kcal/mol of activation barriers. At low temperatures, it is difficult for the hydroxylation to overcome such high barriers. The attack orientation and target also are different from the result obtained by our calculation with DFT/B3LYP method.

In 2000, Uggerud et al. [6(c)] had investigated the unimolecular chemistry of HOOH$_2$$^+$ by the *ab initio* method. They concluded that the most prevalent unimolecular reaction of HOOH$_2$$^+$ is the formation of ^{3}O and H$_3$O$^+$ (Scheme 3). Therefore, the hydroxylation occurs when a triplet oxygen atom is inserted into a C–H bond of hydrocarbon. However, the formation of ^{3}O must overcome 39 kcal/mol (164 kJ/mol) of activation barriers, which makes it equally difficult to explain why the oxidation of alkanes can be completed at very low temperatures.

In 2001, Uggerud et al. [6(d)] obtained a mass spectrum graph with C$_4$H$_9$$^+$ peak after 5.5 s reaction between HOOH$_2$$^+$ and isobutane at 5×10^{-9} mbar. They performed an *ab initio* direct dynamics calculation at the HF/6-31G(d) level on the oxidation of C$_2$H$_6$ + HOOH$_2$$^+$. The calculation obtained a stable system consisting of C$_2$H$_5$$^+$ and two H$_2$O molecules, and the distance between the positive ion and the two H$_2$O is very far. Therefore, they successfully explained the result obtained by mass spectrometry. However, the results are from the experiment and calculation study of unimolecular or bimolecular gas-phase chemistry of protonated hydrogen peroxide. In the *ab initio* cal-

Scheme 2. Distorted methane (Cs) with nonbonding electron pair.

$$^1HOOH_2{}^+ \longrightarrow {}^3O + H_3O^+ \qquad \Delta Ea = 39\ kcal/mol$$

$$^3O + R{-}H \longrightarrow ROH$$

Scheme 3. Mechanism of the hydroxylation by HOOH$_2$$^+$ proposed by Uggerud.

culation of a bimolecular gas-phase reaction, large amounts of energy were deposited in the complex (a thermal insulator), which led in 80% of the trajectories to dissociating into $C_2H_5^+$ and H_2O. We consider that the calculation is unsuitable for liquid-phase reactions, because in condensed systems it is impossible for the energy to be deposited as in bimolecular gas-phase reactions, and so once $C_2H_5^+$ and H_2O are generated, their hydration would be inevitable.

By a DFT based quantum chemical calculation at the B3LYP/6-311G(d,p) level, we found the hydroxylation of alkanes by hydrogen peroxide in superacid is an ionization–hydration process. $HOOH_2^+$ is a superelectrophilic active intermediate because the lowest unoccupied molecular orbital (LUMO) in which the σ^* orbital of its peroxo bond lies has very low energy (−9.18 eV). The energy is at the same level as or even at a lower level than the highest occupied molecular orbital (HOMO) energies of alkanes. Therefore, the activation barriers of the hydroxylation all are very low and might not even exist, which can fully explain why the oxidation of alkane can continue under very low temperature and the oxides often are many and varied. The electrophilic oxygen atom in $HO–OH_2^+$ is the oxygen in the –OH group. The attack target of the oxygen atom is not the C–H bond, nor is it the carbon atom, instead, it is the hydrogen atom of the C–H. For hydroxylation, the σ^* orbital of the peroxo bond of $HOOH_2^+$ is in an important position in the reactions, which is similar to the situation in the epoxidation of alkenes by peracid [7].

2. Method of calculation

The calculation was carried out by using the Gaussian 98 program package [8]. First, both the DFT and *ab initio* methods were tried to calculate the neutral or protonated hydrogen peroxide. We found the calculation with the DFT method could provide more reasonable graphs and energies than with the *ab initio* method. Fig. 1 shows the graphs and energies of the LUMOs of neutral and protonated hydrogen peroxide obtained with DFT at

the B3LYP/6-311G(d,P) level (Fig. 1a and b) and with *ab initio* at the MP4//MP2/6-31g(d,p) level (Fig. 1c and d). In the two graphs obtained with the DFT/B3LYP method, h, i, j and k the four ellipsoids are the typical shapes of an σ^* orbital. Although the two LUMO graphs (Fig. 1a and b) contain some non-σ^* impure component (it is not 100% σ^* orbital), the σ^* orbital of the peroxo bond is major component of the LUMO. Therefore, the $E_{LUMO\sigma^*}$ of the LUMO can reflect and represent the reactivity of the σ^* orbital of the peroxo bond in neutral or protonated HOOH. For Fig. 1c and d, the h in Fig. 1c and the h and k in Fig. 1d already are not ellipsoidal, which indicated that the σ^* orbital of the peroxo bond obtained with *ab initio*/MP$_{2/4}$ contained much more non-σ^* impure component than that obtained with DFT. The graphs obtained with DFT can better display antibonding characteristic of the σ^* orbital than those obtained with *ab initio*. More importantly, the $E_{LUMO\sigma^*}$ (0.21, −9.18 eV) of neutral or protonated hydrogen peroxide obtained with DFT at the B3LYP/6-311G(d,P) level were much lower (∼6 eV) than that (5.95. −2.98 eV) obtained with *ab initio* at the MP4//MP2/6-31G(d,p) level. The $E_{LUMO\sigma^*}$ (−9.18 eV) of $HOOH_2^+$ obtained with DFT was at the same level of E_{HOMO} (−10.8 to −8.0 eV) of alkanes (see Fig. 2), which could explain the origin of alkane oxidation by $HOOH_2^+$. It shows DFT/B3LYP fairly well presented the orbital graphs and the energies of the LUMOs in which the σ^* orbitals of neutral and protonated hydrogen peroxide lie.

The calculation of the LUMO's orbital graphs and energies is in an important position in the study. The reason that the DFT/B3LYP method provides good calculation results is that the method can treat electron correlation energy well and so can effectively calculate the MO's graphs and energies, especially those of antibonding orbital. Therefore, we have selected the DFT/B3LYP method to explore the mechanism of alkane oxidation by HOOH in superacids. In the calculation, geometry optimizations of neutral or protonated hydrogen peroxide and alkanes, the geometries of transition structures, potential energy surface scans (PES) and reaction path calculation (IRC) all were carried out at the B3LYP/6-311G(d,p) level. Obviously,
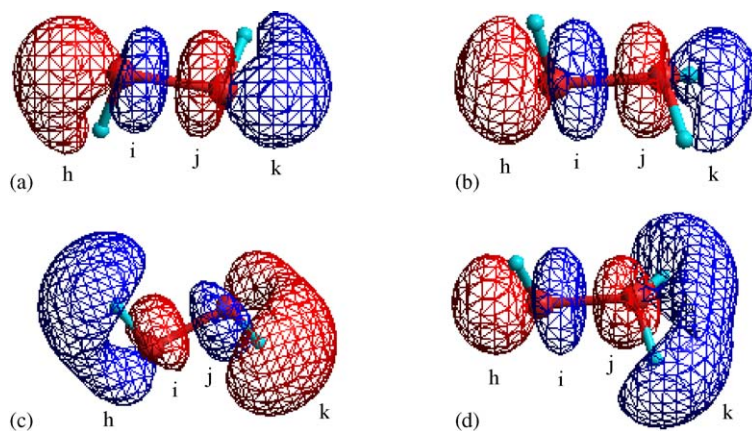

Fig. 1. Graphs and energies of LUMOs of HOOH and $HOOH_2^+$ in which the σ^* orbital of the peroxo bond lies (orbital contour value = 0.06); (a) HOOH $E_{LUMO\sigma^*}$ = 0.21 eV DFT/B3LYP/6-311G(d,p); (b) $HOOH_2^+$ $E_{LUMO\sigma^*}$ = −9.18 eV; DFT/B3LYP/6-311G(d,p); (c) HOOH $E_{LUMO\sigma^*}$ = 5.95 eV *ab initio* MP4//MP2/6-31G(d,p); (d) $HOOH_2^+$ $E_{LUMO\sigma^*}$ = −2.98 eV *ab initio* MP4//MP2/6-31G(d,p).
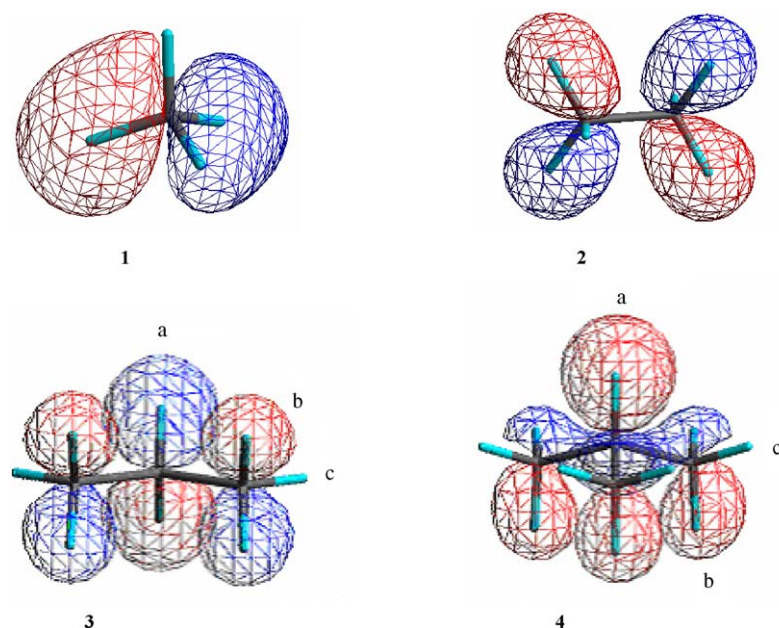
Fig. 2. Graphs and energies of HOMOs of: methane, CH_4 $E_{HOMO} = -10.75$ eV (1); ethane, CH_3CH_3 $E_{HOMO} = -9.40$ eV (2); propane, $CH_3CH_2CH_3$ $E_{HOMO} = -8.97$ eV (3) and isobutene $(CH_3)_3CH$ $E_{HOMO} = -8.80$ eV (4) obtained with DFT at the B3LYP/6-311G(d,p) level (orbital contour value = 0.05).

the same calculation method, level and basis set were used in order to compare the data and reach reliable conclusion.

3. Result and discussion

3.1. Neutral HOOH is unable to complete the hydroxylation of alkanes

The graphs and energies of the HOMOs of three simple alkanes: methane, ethane, propane and one branch chain alkane isobutane obtained with DFT at the B3LYP/6-311G(d,p) level are shown in Fig. 2(1, 2, 3 and 4).

For neutral HOOH, the orbital energy $E_{LUMO\sigma^*}$ of the LUMO obtained using the DFT at the B3LYP/6-311G(d,p) level was 0.21 eV (Fig. 1a). However, the HOMO energies of methane, ethane, propane and isobutane obtained by the same method were -10.75, -9.40, -8.97 and -8.80 eV, respectively. The energies were much lower than the $E_{LUMO\sigma^*}$ of neutral H_2O_2. The differences are all larger than 9 eV (207 kcal/mol). Obviously, the differences were overlarge, which made it difficult for the σ electrons of alkanes to transfer from their HOMO into the LUMO of neutral HOOH.

In order to observe whether the neutral HOOH can oxidize an alkane, a potential energy surface scan (PES) was performed against the extension of the HO–OH bond at the B3LYP/6-311G(d,p) level. The optimized length (1.454 Å) of HO–OH was set as its initial bond distance. The alkane was methane. Calculation results showed that the distances between the two reactants and system energy constantly increase (Table 1, ΔE) along with the extension of the HO–OH bond. At the final site of this scanning, the HO–OH bond distance = 2.454 Å, and the bond had actually disconnected. However, oxidation had not occurred, which indicated HOOH does not have any oxida-

tion reactivity on methane. Some data is shown in Table 1 and Fig. 3.

3.2. Protonation has greatly increased the reactivity of hydrogen peroxide

When HOOH has changed into a protonated positive ion $HOOH_2^+$, the $E_{LUMO\sigma^*}$ of the LUMO in which the σ^* orbital of its peroxo bond lies is much lower than that of the neutral HOOH. The $E_{LUMO\sigma^*}$ of $HOOH_2^+$ obtained by DFT at the B3LYP/6-311G(d,p) level was -9.18 eV (Fig. 1b), which is 9.39 eV lower than that of neutral HOOH. Therefore, the $E_{UMO\sigma^*}$ of the protonated $HOOH_2^+$ is at the same or even a lower level than the HOMO energy of alkanes, which makes nucleophilic attack of the σ electrons in the HOMO of alkanes toward the σ^* orbital of peroxo bonds is easily initiated.

Among the above alkanes, methane has the lowest HOMO energy (-10.75 eV). The energy is 1.57 eV lower than $E_{LUMO\sigma^*}$ of $HOOH_2^+$ and thus the reaction temperature of the hydroxylation of methane by hydrogen peroxide in superacids is the highest, at 0–60 °C [3(a)]. Ethane has the secondary-lowest HOMO energy (-9.40 eV) and is 0.22 eV lower than that of $HOOH_2^+$. Therefore, the reaction temperature of ethane could be lower than that of methane. The experiment indicated the reaction occurred at -40 °C [3(a)]. For propane and *tert*-butane, their

Table 1
The distances O(8)···H(2) between HOOH and methane and the change (ΔE) of system energies along with extension of the HO–OH bond

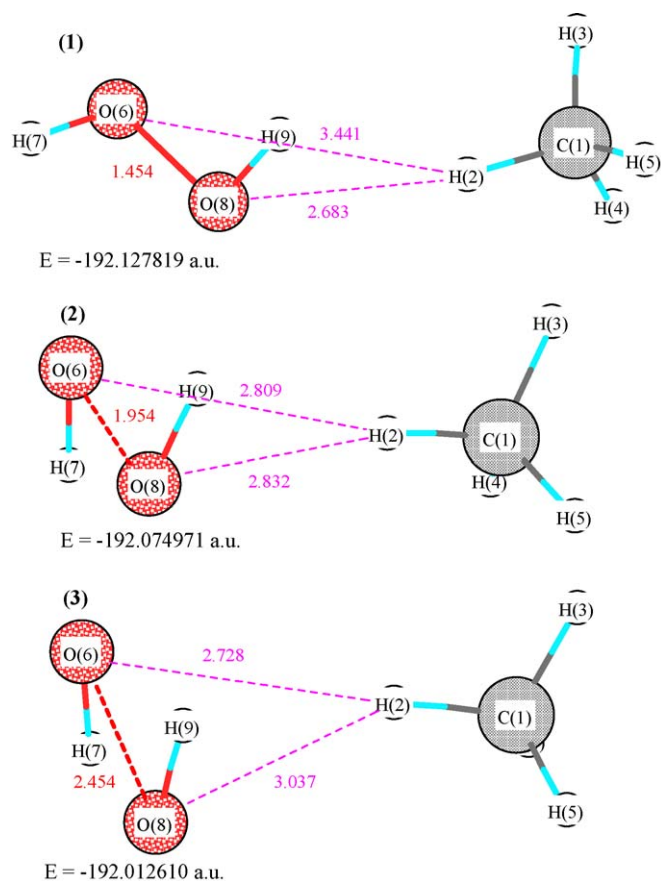| HO–OH (Å)	1.454	1.654	1.854	2.054	2.254	2.454
O(8)···H(2) (Å)	2.683	2.674	2.730	2.821	2.867	3.037
ΔE (kcal/mol)	0	8.29	24.33	41.90	58.23	72.26

Fig. 3. Distances between the HOOH and methane are increasingly farther and the energy of the system constantly rises along with the extension of the HO–OH bond. (1) $E = -192.127819$ a.u.; (2) $E = -192.074971$ a.u.; (3) $E = -192.012610$ a.u.

Fig. 4. CH_4–$HOOH_2^+$ initial structure (cluster-1) and its transition structure (TS-1) obtained by DFT calculation at the B3LYP/6-311G (d,p) level. In the figure, distances are in angstroms, and angles are in degrees.

E_{HOMO} obtained in the calculation was -8.97 and -8.80 eV, respectively (Fig. 2). The energy of the former was 0.21 eV higher than the $E_{LUMO\sigma*}$ of $HOOH_2^+$, that of the latter was 0.38 eV higher than the $E_{LUMO\sigma*}$ of $HOOH_2^+$. Therefore, propane and *tert*-butane could be oxidized at $-78\,°C$.

The order of E_{HOMO} of the alkanes in Fig. 2 is isobutane > propane > ethane > methane. Therefore, the relative order of reactivity of the alkanes on $HOOH_2^+$ obtained by Olah [3(a)] is entirely consistent with the E_{HOMO} order.

3.3. Hydroxylation of methane and ethane: transition structure and activation barrier

According to Olah's experimental results, the main products of the reaction of methane and ethane with HOOH in superacids are methanol and ethanol, i.e., they have been hydroxylated. Among simple alkanes, methane has the lowest HOMO energy
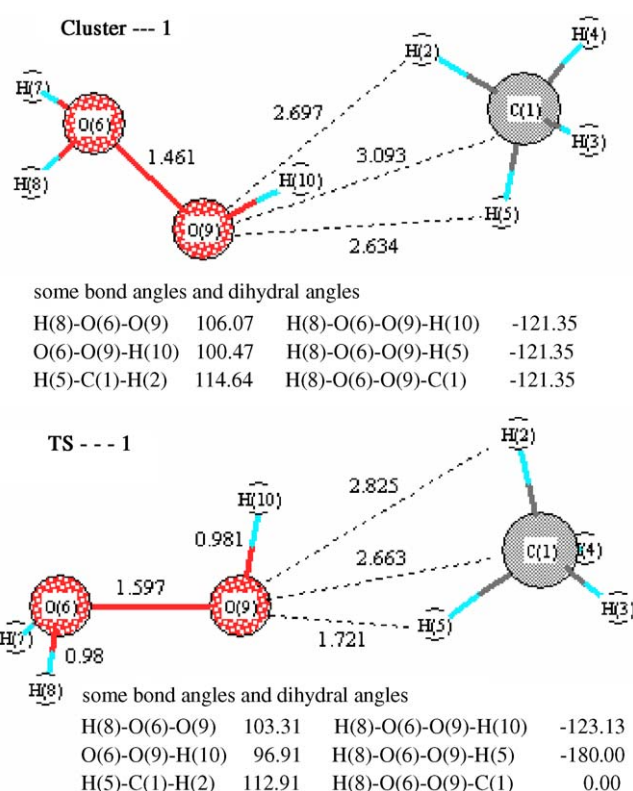
(-10.75 eV) and thus its hydroxylation should have the highest activation barrier. Ethane has the secondary-lowest HOMO energy (-9.40 eV) and thus its activation barrier should be lower than methane. The E_{HOMO} order of the alkanes tallies with the activation barriers obtained by the calculation at the B3LYP/6-311G(d,p) level. The activation barriers of methane and ethane are 2.58 and 1.40 kcal/mol, respectively. Therefore, the reactivity of the both displayed an evident difference. Their activation barriers, initial cluster and transition structure are shown in Table 2 and Figs. 4 and 5. The initial structures cluster-1, cluster-2 and energies $E_{cluster}$ are from IRC and then Opt calculation.

3.4. Microscopic process and mechanism of the hydroxylation

In order to observe the microscopic process of the alkane hydroxylation, a reaction path calculation (IRC) of $HOOH_2^+$ on methane was performed. We listed some representative results from the IRC (Table 3 and Fig. 6), which were enough to display the nature of the hydroxylation.

Table 2
Activation barriers of hydroxylation of methane, ethane by $HOOH_2^+$ obtained from their electronic energies (E_{TS}, $E_{cluster}$)

E_{TS} (a.u.)	ZPE_{TS} (a.u.)	$E_{cluster}$ (a.u.)	$ZPE_{cluster}$ (a.u.)	ΔE^* (kcal/mol)
-192.399977	0.082850	-192.404085	0.085356	2.58 (1.01)
-231.726618	0.113473	-231.728849	0.114874	1.40 (0.52)

The data in brackets has considered the zero-point correction energies (ZPE_{TS}, $ZPE_{cluster}$).
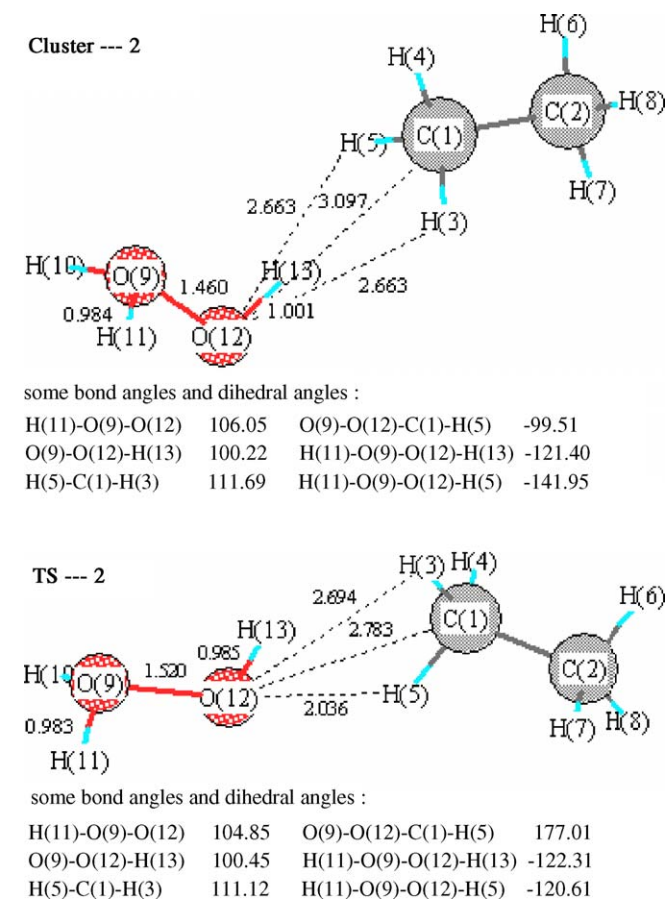
Fig. 5. CH_3CH_3–$HOOH_2^+$ initial structure (cluster-2) and its transition structure (TS-2) obtained by DFT calculation at the B3LYP/6-311G (d,p) level. In the figure, distances are in angstroms, and angles in degrees.

The data in Table 3 show the total charges on methane in the intermediates all were positive, which proved the transfer of σ-electrons on C–H bond of methane toward the σ* orbital of the peroxo bond occurs. The quantity of the electron transfer in Table 3 increases along with the spread of the HO–OH_2^+ bond. In the light of a large number of chemical experiments, σ-electrons of C–H bonds of alkanes are very stable in common chemical reactions. However, $HOOH_2^+$ can easily capture the σ-electrons of alkanes, which shows the protonated hydrogen peroxide is an extraordinary superelectrophilic active intermediate.

Fig. 6 shows the HOMO graphs of the initial structure and some marked intermediates (including TS) obtained by IRC, Opt and single point energy calculations.

Table 3
From IRC and single point energy calculation, σ-electrons on –C–H bonds of methane have transferred into the σ* orbital of the peroxo bond of H_2OOH^+

H_2O–OH^+ (Å)	Total charge on methane
1.463	0.077
1.538	0.117
1.597 (TS)	0.182
1.717	0.328
1.947	0.590

1: shows HOMO graph of the initial structure obtained by the IRC and Opt calculation. Although the total Mulliken atomic charge of methane is not 0 in the initial structure, the electrons of methane were not transferred into the σ* orbital of the peroxo bonds of $HOOH_2^+$ and by comparison the charge quantity is small.

2: σ-electrons of methane begins to transfer into the σ* orbital of the peroxo bond of $HOOH_2^+$.

3: TS has formed. The σ-electron transfer of methane toward the σ* orbital has increased.

4 and 5: The σ-electrons transfer continuously increased along with the spread of O–O bond distance. The hydrogen atom of –C–H bond was gradually approaches to the oxygen atom of –O–H in $HOOH_2^+$, i.e., according to classical concept a hydride (H^-) is being transferred.

6: At this moment, the $HOOH_2^+$ and methane have changed into one positive ion of the methyl group and two water molecules, which means the hydride (H^-) has transferred to $HOOH_2^+$.

7: The H_2O moves toward the carbon atom in H_3C^+.

8: The hydration of H_2O and H_3C^+ has finally produced protonated methanol. In acidic medium, alcohol is present in the protonated state, which is reasonable.

For 2–5 in Fig. 6, among h, i, j and k the four ellipsoidals of the σ* orbital of H_2OOH^+ (see Fig. 1), h, i and j have appeared, but k has not appeared. It shows an overlap of the HOMO of methane with the σ* orbital of $HOOH_2^+$ occurred. In addition, h, i and j originally are a part of the empty σ* orbital (main component of the LUMO of $HOOH_2^+$), but now have changed into a part of the HOMO of the systems. This proved that the σ-electrons of methane were transferred into the σ* orbital of $HOOH_2^+$. The bulk of h, i and j have grown in size, but the orbital bulk on methane decreased somewhat along with the extension of the HO–OH_2^+ bond. This shows the transfer quantity of σ-electrons of methane increased. We believe the transfer already has been completed when $HOOH_2^+$ has changed into two H_2O molecules in Fig. 6(6).

Olah, Alder and Whiting suggested the hydroxylation of alkanes should be attributed to the protonation of hydrogen peroxide. This conclusion is consistent with above the calculation results. However, they considered that the hydroxylation was completed through a pentacoordinated carbocation [3,9] (Scheme 1, TS). The calculation result from IRC indicated the active oxygen atom in the –O–H group of $HOOH_2^+$ attacked neither the carbon atom of the –C–H bond nor the –C–H bond of methane, but attacked the hydrogen atom of the –C–H bond. The oxygen atom in the –O–H group of $HOOH_2^+$ was not coordinated with the carbon atom of methane and thus the so-called pentacoordinated carbocation had not formed.

In light of the above results, the mechanism of the hydroxylation of alkanes by hydrogen peroxide in superacids is an ionization–hydration process. The proposed mechanism is shown in Scheme 4.

The alkanes were first ionized into a carbocation, and meanwhile $HOOH_2^+$ was changed into two H_2O molecules. Then the hydration of the carbocation with a H_2O has produced a protonated alcohol. Of course, the protonation on HOOH is the key of
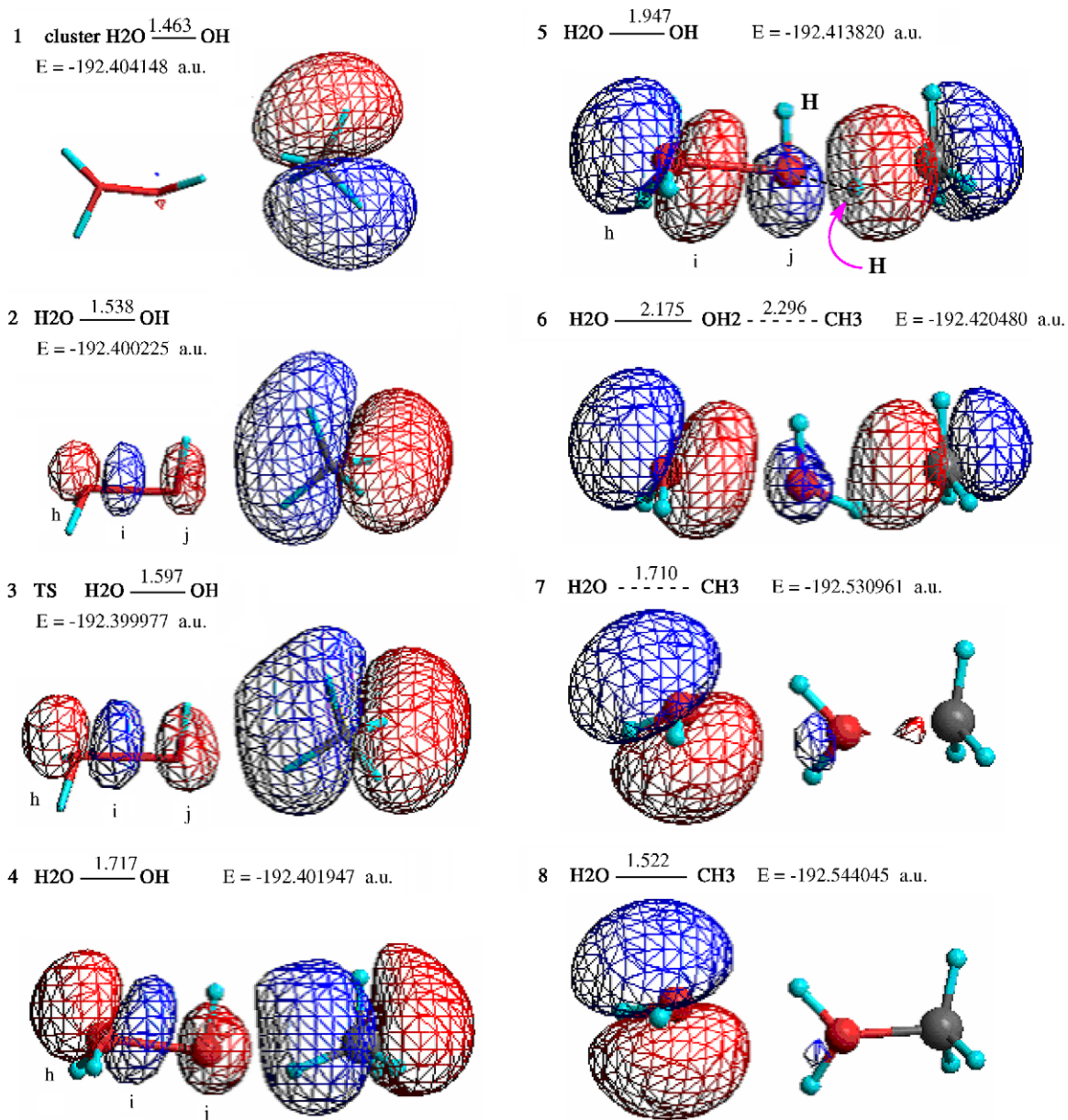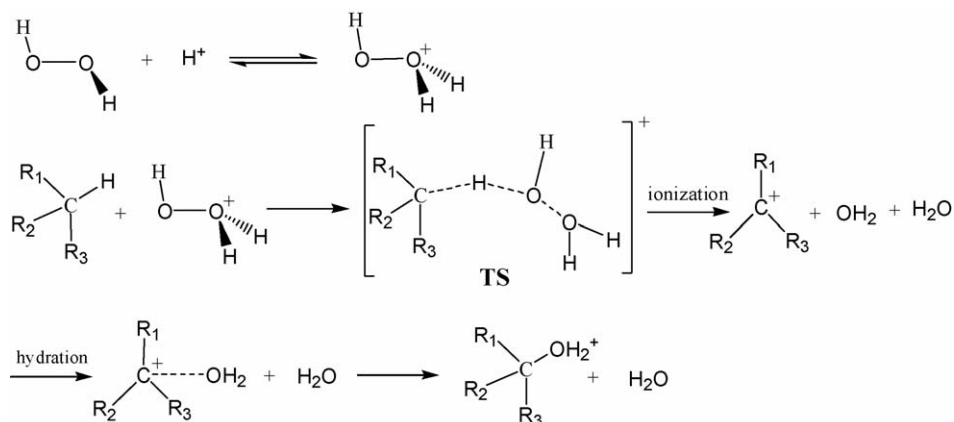
Fig. 6. HOMO graphs of initial structure 1, intermediates 2–7 (3 is TS) and product 8 in the hydroxylation. 1 and 8 were obtained by IRC and Opt calculation, 2–7 by IRC and single point energy calculations (orbital contour value = 0.03).

Scheme 4. Proposed mechanism on the hydroxylation of alkanes by HOOH in superacid. The optimized structure of neutral HOOH is not a plane.
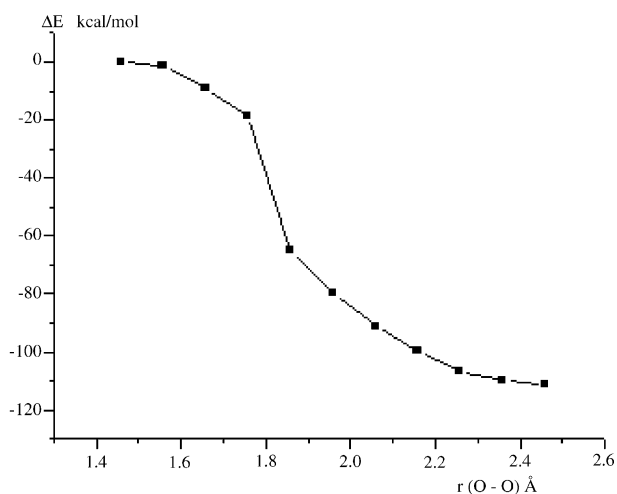
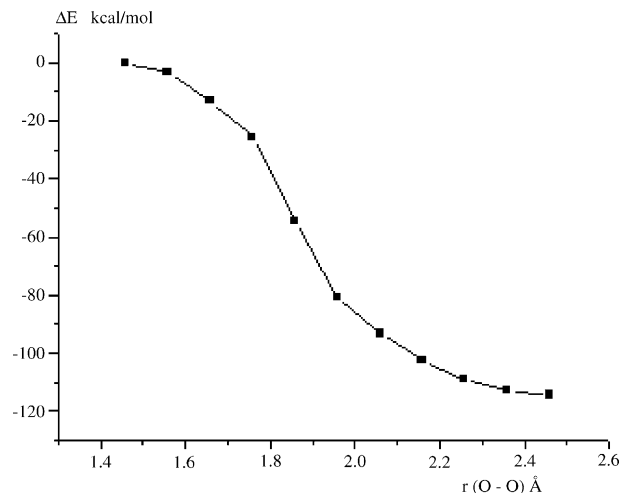Fig. 7. The hydroxylation of the secondary carbon atom of propane by $HOOH_2^+$ is a spontaneous process.

Fig. 8. The hydroxylation of the tertiary carbon atom of isobutane by $HOOH_2^+$ is a spontaneous process.
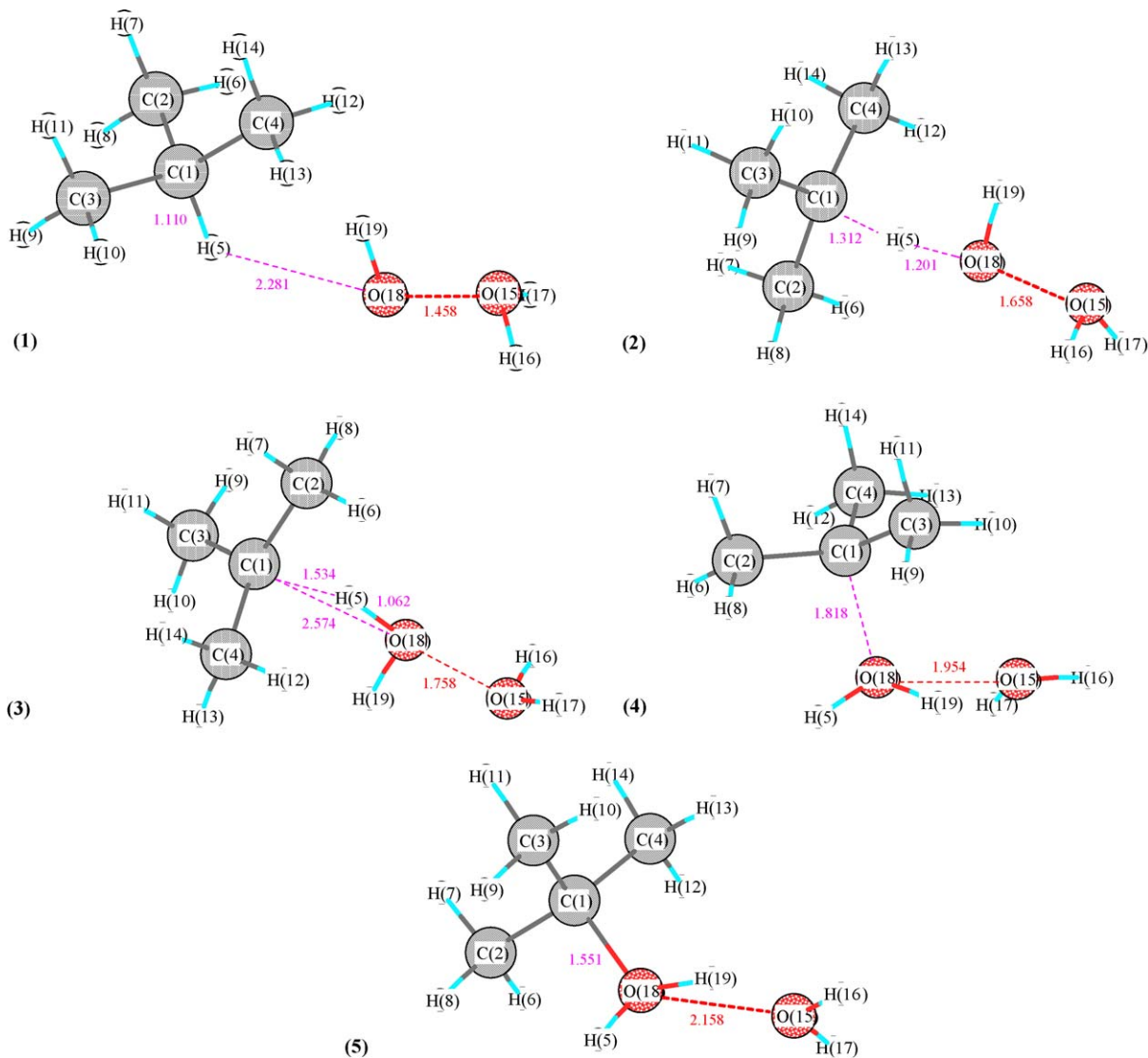

Fig. 9. The hydroxylation of tertiary carbon atoms of isobutane is a spontaneous process, but also is an ionization–hydration process. (1) The initial structure of the scanning system. O[18] is toward H[5]; (2) O[18] attacks H[5]. C[1]–H[5] bond approximately has disconnected, the tertiary hydrogen atom H[5] is moving toward O[18] of $HOOH_2^+$; (3) H[5] with O[18] has bonded, two H_2O molecules and one $(CH_3)_3C^+$ have formed; (4) O[18] is moving toward to C[1]. The distance between two water molecules is longer; (5) O[18] with C[1] has bonded. Thus, the products are a protonated *tert*-butanol molecule and a H_2O molecule.

the reaction because it makes HOOH has changed into a super-electrophilic active intermediate. The microscopic nature of the hydroxylation is nucleophilic transfer of σ-electrons of alkanes toward the σ^* orbital of the proxo bond of $HOOH_2^+$. It seems the nucleophilic transfer of substrate electrons toward the σ^* orbital of peroxo bond is a general rule for the oxidations of using the peroxides with the peroxo bond (O–O). The electrons may be π electrons [7], or may be σ or other electrons.

3.5. Hydroxylation of secondary carbon and tertiary carbon: a spontaneous process

Oxidation (not only hydroxylation) of propane and isobutane by $HOOH_2^+$ easily occur, even at −78 °C, which indicates their reactivity is much higher than methane and ethane. Propane has primary and secondary carbon atoms and isobutane has primary and tertiary carbon atoms. According to the optimized conformation and the electron population of HOMO in Fig. 2(3 and 4), the –C–H σ bonds a in propane and isobutane molecules occupy a greater part of the electron cloud in the HOMO. Since the hydroxylation is a nucleophilic transfer of σ electrons of the C–H bond toward the σ^* orbital of peroxo bonds in $HOOH_2^+$, according to the electron population of the HOMOs, the reactivity of a should be the highest. For b and c, the population of the two σ electrons in the HOMO is small or not present. Therefore,

Table 4
Some scanning results on the hydroxylation of secondary carbon atom of propane: total energy (E) and energy difference (ΔE) obtained by scanning of each step 0.1 Å at B3LYP/6-311G(d,p) level

No.	$H_2O–OH^+$	E (a.u.)	ΔE (kcal/mol)
0	1.458	−271.053775	0.00
1	1.558	−271.056106	−1.46
2	1.658	−271.067927	−8.88
3	1.758	−271.083389	−18.57
4	1.858	−271.157610	−65.12
5	1.958	−271.180526	−79.49
6	2.058	−271.198906	−91.02
7	2.158	−271.212944	−99.83
8	2.258	−271.223574	−106.50
9	2.358	−271.229034	−109.92
10	2.458	−271.230947	−111.12

their reactivity does not mainly depend on the population of the two electrons in HOMO. Because σ electrons on the C–H bonds of b and c mainly are in the orbital with lower energy than that of HOMO, their reactivity is certainly lower than a. Actually, under normal reaction condition, the –CH_3 group is in rotation, and thus the reactivity of the three C–H bond in –CH_3 is equal.

In order to observe the hydroxylation process on secondary carbon atoms of propane and tertiary carbon atom of isobutane
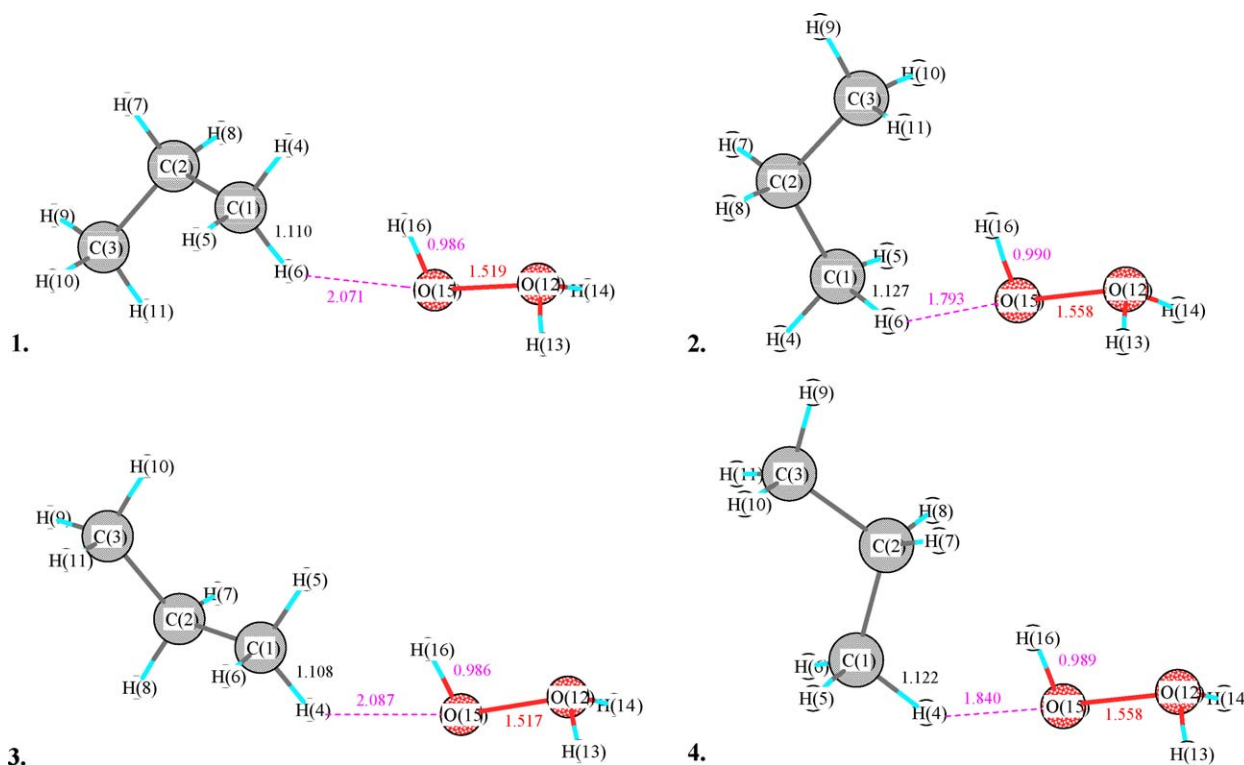

Fig. 10. The transition structures and activation barrier of the attacks of $HOOH_2^+$ toward hydrogen atoms b and c of propane obtained by DFT calculation at the B3LYP/6-311G(d,p) level. In the figures, distances are in angstroms. (1) For the attack orientation of $HOOH_2^+$ toward hydrogen atoms b, the total energies of the TS and its cluster are −271.052130 and −271.054319 a.u., respectively. The activation barrier is 1.37 kcal/mol. (2) For the attack orientation of $HOOH_2^+$ toward hydrogen atoms b, the total energies of the TS and its cluster are −271.054577 and −271.054719 a.u., respectively. The activation barrier is 0.09 kcal/mol. (3) For the attack orientation of $HOOH_2^+$ toward hydrogen atoms c, the total energies of the TS and its cluster are −271.052235 and −271.054316 a.u., respectively. The activation barrier is 1.31 kcal/mol. (4) For another attack orientation of $HOOH_2^+$ toward hydrogen atoms c, the total energies of TS and its cluster are −271.052882 and −271.053946 a.u., respectively. The activation barrier is 0.67 kcal/mol.

Table 5
Some scanning results on hydroxylation of the tertiary carbon atom of isobutane: total energy (E) and energy difference (ΔE) obtained by the scanning of each step 0.1 Å at the B3LYP/6-311G(d,p) level

No.	$H_2O–OH^+$	E (a.u)	ΔE (kcal/mol)
0	1.458	−310.379964	0.00
1	1.558	−310.385467	−3.45
2	1.658	−310.400902	−13.13
3	1.758	−310.420701	−25.55
4	1.858	−310.482360	−54.78
5	1.958	−310.508540	−80.64
6	2.058	−310.528793	−93.34
7	2.158	−310.543902	−102.82
8	2.258	−310.554115	−109.23
9	2.358	−310.560155	−113.01
10	2.458	−310.562579	−114.53

by $HOOH_2^+$, a potential energy surface scan (PES) was performed as described in Section 1. Here the initial bond distance of the 2 oxygen atoms in $HO–OH_2^+$ is the optimized length (1.458 Å) obtained by DFT at the B3LYP/6-311G(d,p) level and 10 scan steps of 0.1 Å each were carried out.

For secondary carbon atoms of propane and tertiary carbon atom of isobutane, some results of the PES scanning are shown in Tables 4 and 5. According to the total energy (vertical axes) of each scanning step and the distance (horizontal axes) between the two oxygen atoms in $HO–OH_2^+$, a potential energy curve of the hydroxylation of propane and isobutane are shown in Figs. 7 and 8, respectively.

The tables and figures show that the total energy of the bimolecular system decreases all the time along with the extension of the peroxo bond. Therefore, the hydroxylation by $HOOH_2^+$ is a spontaneous reaction because a barrier does not appear. Therefore, propane and isobutane can be easily oxidized by $HOOH_2^+$ at −78 °C. This phenomenon obviously is reasonable because H_2O_2 is protonated into the $HOOH_2^+$ at once, and the hydroxylation or other oxidation reactions do not need to overcome any barriers.

The potential energy surface scanning (PES) by DFT calculation at the B3LYP/6-311G(d,p) level also vividly depicts the process of the hydroxylation. Although activation barriers do not exist, the hydroxylation of secondary carbon atom of propane and tertiary carbon atom of isobutane also undergo the same ionization–hydration process as methane and ethane. Fig. 9 displays the hydroxylation process of isobutane by several marked scanning steps. The process of propane is similar to that of isobutane.

3.6. Hydroxylation of primary carbon in propane and isobutane: transition structure and activation barrier

For the hydroxylation of primary carbon atoms of propane and isobutane, the reaction must overcome activation barriers, i.e., it is not a spontaneous process. According to different orientations, the attacks of $HOOH_2^+$ toward the hydrogen atoms would have several transition structures. For the attack toward

b and c hydrogen atoms (see Fig. 2(3)) of propane, we already have obtained four transition structures. Their activation barrier are 1.39, 0.09, 1.31 and 0.67 kcal/mol (Fig. 10(1, 2, 3 and 4)), respectively. For the attack toward b and c hydrogen atoms (see Fig. 2(4)) of isobutane, we have obtained two transition structure (Fig. 11(1 and 2)). The barriers are 0.11, 1.21 kcal/mol, respectively (none of the barriers included their ZPE). However, the methyl groups are in continuous rotation. Therefore, the activation barriers of the hydroxylation on the primary carbon atoms of propane and isobutane should roughly be in the range of 0.1–1.4 kcal/mol. The data confirmed the activation barriers of hydroxylation on the primary carbon atoms are very low. Therefore, the primary carbon atoms also can be oxidized in the reaction. Olah's experiments [3(a)] show that the products of oxidation by $HOOH_2^+$ are many and varied. The origin should be attributed to the fact that the activation barriers of oxidation by the superelectrophilic $HOOH_2^+$ on alkanes or intermediate products are very low or even do not exist. The transition structure and activation barrier are shown in Figs. 10 and 11, respectively. Their initial structures have been left out and ZPE has not been included.
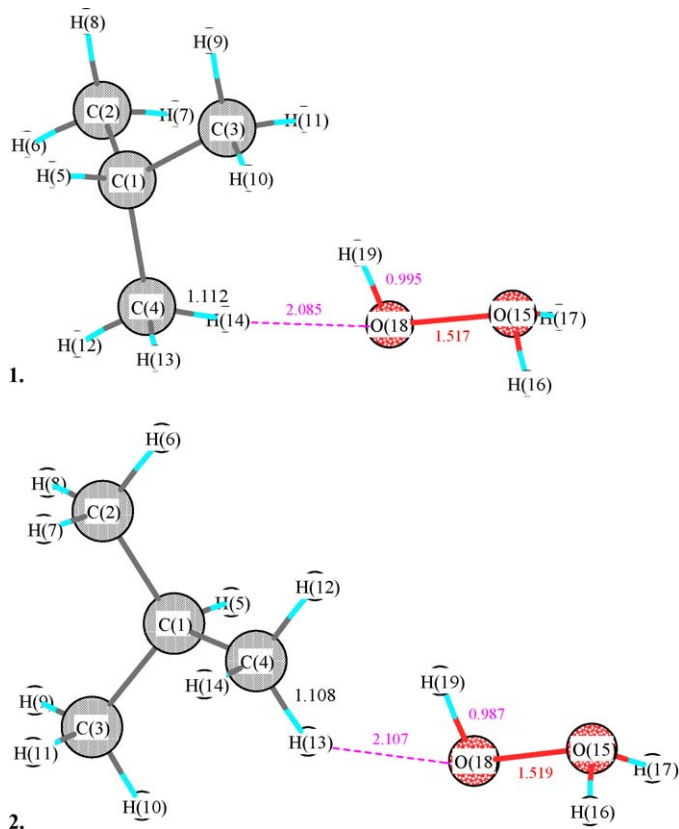

Fig. 11. The transition structures and activation barrier of the attacks of $HOOH_2^+$ toward hydrogen atoms b and c of isobutane obtained by DFT calculation at the B3LYP/6-311G(d,p) level. In the figures, distances are in angstroms. (1) For the attack direction of $HOOH_2^+$ toward hydrogen atoms b, the total energies of the TS and its cluster are −310.380756 and −310.380588 a.u., respectively. The activation barrier is 0.11 kcal/mol. (2) For attack direction of $HOOH_2^+$ toward hydrogen atoms c, the total energies of TS and its cluster are −310.380115 and −310.378193 a.u., respectively. The activation barrier is 1.21 kcal/mol.

4. Conclusion

The calculation with DFT at the B3LYP/6-311G(d,p) level has proved:

(1) The protonation of HOOH in superacid is the key to oxidation because it has produces the superelectrophilic active intermediate ($HOOH_2^+$). The superelectrophilic property of $HOOH_2^+$ can be attributed to the fact that its σ^* orbital of peroxo bond has very low energy (-9.18 eV). The energy is at approximately the same, or even a lower level than the HOMO energy of alkanes, which makes nucleophilic transfer of σ-electrons of alkanes toward the σ^* orbital of peroxo bond has easily initiated.

(2) The electrophilic oxygen atom in $HO–OH_2^+$ is the oxygen in the –OH group. The attack target of the oxygen atom is the hydrogen atom of C–H. $HOOH_2^+$ can capture the σ electrons on C–H of alkanes and then take the hydride (H^-), which makes the alkane change into a carbocation and causes $HOOH_2^+$ to divide into two H_2O molecules. Soon after that, the hydration of an H_2O molecule with the carbocation takes place and finally protonated alcohol is formed. Therefore, the hydroxylation follows an ionization–hydration pathway (Scheme 4). The microscopic nature of the ionization is nucleophilic transfer of σ-electrons of alkanes toward the σ^* orbital of peroxo bond of $HOOH_2^+$.

(3) The calculation results on methane, ethane, propane and isobutane show the activation barriers of the hydroxylation of alkanes by $HOOH_2^+$ is either very low or not present. Therefore, the hydroxylations are approximately or entirely spontaneous reactions. The results can explain why alkanes could be oxidized by hydrogen peroxide in superacid at low temperature, even at $-78\,^\circ$C and form many and varied products.

References

[1] R.W. Alder, M.C. Whiting, J. Chem. Soc. (1964) 4707.
[2] U. Frommer, Z. Ullrich, Naturforsch B 26 (1971) 332.
[3] (a) G.A. Olah, D.G. Parker, N. Yoneda, Angrew. Chem. Ed. Engl. 17 (1978) 909;
    (b) G.A. Olah, D.G. Parker, N. Yoneda, Angrew. Chem. Ed. Engl. 21 (1982) 734;
    (c) G.A. Olah, N. Hartz, G. Rasul, G.K.S. Prakash, J. Am. Chem. Soc. 117 (1995) 1336.
[4] J.O. Edwards, in: J.O. Edwards (Ed.), Peroxide Reaction Mechanisms, Wiley, New York, 1962, pp. 67–106.
[5] (a) P.R. Schreiner, P.V.R. Schleyer, H.F. Schaefer, J. Am. Chem. Soc. 115 (1993) 9659;
    (b) A.A. Fokin, P.R. Schreiner, Chem. Rev. 102 (2002) 1551.
[6] (a) R.D. Bach, J.I. Andres, M.D. Su, J.J. MeDouall, J. Am. Chem. Soc. 115 (1993) 5768;
    (b) R.D. Bach, M.D. Su, J. Am. Chem. Soc. 116 (1994) 10103;
    (c) E.L. Qistad, J.N. Harvey, E. Uggerud, J. Phys. Chem. A 104 (2000) 8382;
    (d) Å.M.L. Øistad, A.C. Petersen, V. Bakken, J. Vedde, E. Uggerud, Angrew. Chem. Int. Ed. 40 (7) (2001) 1305.
[7] H.C. Shi, Z.G. Zhang, Y.L. Wang, J. Mol. Catal. A: Chem. 238 (2005) 13.
[8] M.J. Frisch, G.W. Trucks, H.B. Schlegel, G.E. Scuseria, M.A. Robb, J.R. Cheeseman, V.G. Zakrzewski, J.A. Montgomery Jr., R.E. Stratmann, J.C. Burant, S. Dapprich, J.M. Millam, A.D. Daniels, K.N. Kudin, M.C. Strain, O. Farkas, J. Tomasi, V. Barone, M. Cossi, R. Cammi, B. Mennucci, C. Pomelli, C. Adamo, S. Clifford, J. Ochterski, G.A. Petersson, P.Y. Ayala, Q. Cui, K. Morokuma, D.K. Malick, A.D. Rabuck, K. Raghavachari, J.B. Foresman, J. Cioslowski, J.V. Ortiz, A.G. Baboul, B.B. Stefanov, G. Liu, A. Liashenko, P. Piskorz, I. Komaromi, R. Gomperts, R.L. Martin, D.J. Fox, T. Keith, M.A. Al-Laham, C.Y. Peng, A. Nanayakkara, M. Challacombe, P.M.W. Gill, B. Johnson, W. Chen, M.W. Wong, J.L. Andres, C. Gonzalez, M. Head-Gordon, E.S. Replogle, J.A. Pople, Gaussian 98, Revision A.9, Gaussian Inc., Pittsburgh, PA, 1998.
[9] (a) G.A. Olah, Chem. Br. 8 (1972) 281;
    (b) G.A. Olah, Chem. Tech. 1 (1971) 566.